Electronic Supplementary Material (ESI) for Journal of Materials Chemistry C.

Electronic Supplementary Information

Understanding the efficiency drooping of blue organometallic phosphors: a computational study of radiative and non-radiative decay rates for triplets

Qian Peng, Qinghua Shi, Yingli Niu, Yuanping Yi,* Shaorui Sun, Wenqiang Li, Zhigang Shuai*

Contents

I. Methodology

i) Radiative Decay Rate Constant and Emission Spectrum.

The radiative decay rate constant was calculated by integrating over the whole emission spectrum,

$$k_r(T) = \int \sigma_{em}(\omega, T) d\omega \tag{S-1}$$

$$\sigma_{em}(\omega, T) = \frac{4\omega^3}{3\hbar c^3} \sum_{u,v} P_{iv}(T) \left| \left\langle \Theta_{fu} \left| \vec{\mu}_{fi} \right| \Theta_{iv} \right\rangle \right|^2 \delta\left(\omega_{iv,fu} - \omega\right) \tag{S-2}$$

Here P_{iv} is the Boltzmann distribution function of the initial state at certain temperature; Θ is the nuclear vibrational wave function. $\vec{\mu}_{fi} = \left\langle \Phi_f \left| \vec{\mu} \right| \Phi_i \right\rangle$ is the electric transition dipole moment between two electronic states.

By applying the fourier transformation for the delta function, the Eq. (2) can be written as the form of thermal vibration correlation function,

$$\sigma_{em}(\omega, T) = \frac{4\omega^3}{3\hbar c^3} \left| \mu_0 \right|^2 \int_{-\infty}^{\infty} \mathrm{d}t e^{i(\omega - \omega_{fi})t} \left[Z_i^{-1} \rho_{em}(t, T) \right] \tag{S-3}$$

$$\rho_{em}(t, T) = \mathrm{Tr}\left[e^{-i\tau_f \hat{H}_f} e^{-i\tau_i \hat{H}_i} \right] \tag{S-4}$$

Analytical solution to Eq. (4) can be obtained by virtue of Gaussian integration.

ii) Non-radiative Decay Rate Constants

Based on the time-dependent perturbation theory and Born-Oppenheimer adiabatic approximation, the thermal average rate constant from the initial electronic state i with the vibrational quantum numbers *v* to the final electronic state f with the vibrational quantum numbers *u* reads:

$$k_{\mathrm{f}\leftarrow\mathrm{i}}=\frac{2\pi}{\mathrm{h}}\sum_{v_{\mathrm{i}},v_{\mathrm{f}}}P_{\mathrm{i}v_{\mathrm{i}}}\left|H'_{\mathrm{f}v_{\mathrm{f}},\mathrm{i}v_{\mathrm{i}}}+\sum_{n,v_{\mathrm{n}}}\frac{H'_{\mathrm{f}v_{\mathrm{f}},nv_{\mathrm{n}}}H'_{nv_{\mathrm{n}},\mathrm{i}v_{\mathrm{i}}}}{E_{\mathrm{i}v_{\mathrm{i}}}-E_{nv_{\mathrm{n}}}}\right|^{2}\delta\left(E_{\mathrm{i}v_{\mathrm{i}}}-E_{\mathrm{f}v_{\mathrm{f}}}\right), \tag{S-5}$$

H' denotes the interaction between two different Born-Oppenheimer states, consisting of two contributions:

$$\hat{H}'\Psi_{\mathrm{i}v_{\mathrm{i}}}=\hat{H}^{\mathrm{BO}}\Phi_{\mathrm{i}}\left(\mathbf{r};\mathbf{Q}\right)\Theta_{\mathrm{i}v_{\mathrm{i}}}\left(\mathbf{Q}\right)+\hat{H}^{\mathrm{SO}}\Phi_{\mathrm{i}}\left(\mathbf{r};\mathbf{Q}\right)\Theta_{\mathrm{i}v_{\mathrm{i}}}\left(\mathbf{Q}\right) \tag{S-6}$$

where $\hat{H}^{\mathrm{BO}}$ is the non-adiabatic coupling and H^{SO} is in Eq. (57), and **r** and **Q** are the electronic and normal mode coordinates, respectively.

For the organometallic complex, the spin-orbit coupling elements (>100 cm^{-1}) are much larger than those in pure organic fluorescent molecules (<1.0 cm^{-1}).[20] Therefore, it is reasonable to calculate the non-radiative rate constant (k_{nr}) by using the first-order perturbation rate formula. The intersystem crossing rate constant between two electronic states with different spin state can be expressed as,

$$k_{\mathrm{ISC}}(\omega,T)=\frac{1}{\hbar^{2}}\left|\left\langle\Phi_{\mathrm{f}}\left|\hat{H}^{\mathrm{SO}}\right|\Phi_{i}\right\rangle\right|^{2}\int_{-\infty}^{\infty}\mathrm{d}t\mathrm{e}^{\mathrm{i}\omega_{\mathrm{fi}}t}\left[Z_{\mathrm{i}}^{-1}\rho_{\mathrm{ISC}}(t,T)\right] \tag{S-7}$$

Here $\rho_{\mathrm{ISC}}(t,T)$ is the same thermal vibration correlation function with eq. 4.

All the emssion spectrum, radiative and nonradiative decay rates equation are solved in MOMAP program.

iii) Reorganization energy

The reorganization energy for phosphorescence from the T_1 state to the ground state can be obtained from the adiabatic potential energy surfaces of the ground states:

$$\lambda=E_g(T_1\ geometry)-E_g(S_0\ geometry) \tag{S-8}$$

where $E_g(T_1/S_0\ geometry)$ is the ground-state energy at the T_1/S_0 equilibrium geometry. Under the harmonic oscillator approximation, the reorganization energy can be also expressed as a summation over all the normal modes:

$$\lambda = \sum_{k=1}^{3n-6} \lambda_k = \sum_{k=1}^{3n-6} \frac{1}{2} \omega_k^2 \Delta Q_k^2 = \sum_{k=1}^{3n-6} \hbar \omega_k S_k \quad \text{(S-9)}$$

Here, ω_k represent the frequency of the k^{th} normal mode at the ground state, and S_k and ΔQ_k are the Huang-Rhys factor and the displacement along the k^{th} normal mode coordinate between the equilibrium positions of the ground state and the T_1 state.

II. Tests of Basis Sets

fac-Ir(ppy)$_3$ is a typical Iridium(III) complex applied for OLED. Its geometry is very similar with those of the compounds in this study. Especially there are rich crystal structure data about it. So we firstly optimized the structure of fac-Ir(ppy)$_3$ at the ground state by using the Los Alamos ECP (Lanl2dz) / Stuttgart Dresden ECP (SDD) for Ir(III) and 6-31g*/ 6-31g** for other light atoms and presented the results in Table S1. It can be seen that the Ir-N bonds are always overestimated by all basis sets while SDD is a little better than Lanl2dz; comparatively, the calculated Ir-C bonds are close to the experimental values. Interesting, the Ir-C bonds got by SDD are closer to the experiments in ref.S1 while the Ir-C bonds got by Lanl2dz are in better agreement with the values in ref.S2. Of course, 6-31g** is better than 6-31g* due to considering more basis functions. Therefore, we chose the basis set SDD for Iridium and 6-31g** for other light atoms in all the geometrical and electronic structure calculations for the compounds under study. Then, the spin-orbit coupling matrix elements (SOCME) were evaluated by adopting different basis sets on light atoms (H, C and N) in Ir(ppz)$_2$(ppy) (see Table S2). The results indicate that 6-31G** is the best choices when considering the balance between computational cost and accuracy. We further compared SOCME and the transition dipole moment elements μ computed with Lanl2dz and SDD for Iridium coupled with 6-31G** for other atoms in Table S3. From Table S3, it can be seen that both SOC and μ got by Lanl2dz are smaller than those of SDD. Furthermore, we compared the radiative rate constants based on the electronic structure information and the transition dipole moment got by Lanl2dz/6-31g** and SDD/6-31g**

respectively and found the latter is much closer to the experiments. Therefore, all the electronic structure and properties calculations were performed by using SDD for Ir atom and 6-31G** for other atoms in this paper.

S1. J. Breu, P. Stossel, S. Schrader, A. Starukhin, W. J. Finkenzeller, H. Yersin, *Chem. Mater.* **2005**, *17*, 1745.

S2. F. Garces, K. Dedeian, N. Keder, R. Watts, *Acta Crystallogr., Sect. C: Cryst. Struct. Commun.* **1993**, *49*, 1117.

Table S1. Calculated bond lengths (Å) in the optimized ground state (the numbers in parentheses denote the various ppy ligands).

	Lanl2dz /6-31g*	SDD /6-31g*	Lanl2dz /6-31g**	SDD /6-31g**	Expt[a)]	Expt[b)]
Ir-N(1)	2.1893	2.1890	2.1903	2.1895	2.086	2.132
Ir-C(1)	2.0270	2.0359	2.0269	2.0363	2.034	2.024
Ir-N(2)	2.1904	2.1883	2.1887	2.1884	2.086	2.132
Ir-C(2)	2.0267	2.0358	2.0264	2.0358	2.034	2.024
Ir-N(3)	2.1906	2.1886	2.1888	2.1870	2.086	2.132
Ir-C(3)	2.0275	2.0364	2.0269	2.0355	2.034	2.024

Notes: [a)] reference S1; x ray; [b)] reference S2, x ray.

Table S2. Calculated Spin-orbit coupling elements (cm^{-1}) for **1** with B3LYP LR method with different basis sets on light atoms and SDD on Ir atom.

	ΔE /eV	$\langle S_0 \lvert \hat{H}^{SO} \rvert T_{1,x} \rangle$	$\langle S_0 \lvert \hat{H}^{SO} \rvert T_{1,y} \rangle$	$\langle S_0 \lvert \hat{H}^{SO} \rvert T_{1,z} \rangle$
6-31G	2.6293515	86.512075	-323.05929	-129.44728
6-31G*	2.6407824	97.349169	-262.81030	-118.55504
6-31G**	2.6378751	96.594965	-263.41643	-118.51061
6-311G*	2.6255673	93.748804	-257.52820	-116.37100

Table S3. Calculated spin-orbit coupling (SOC) and transition dipole moments of 1 from T_1 to S_0 using Lanl2dz/SDD on Ir atoms and 6-31G** on other atoms (C, H, N and F)

	Lanl2dz	SDD
SOC	x: 98.43 cm^{-1} y: -256.83 cm^{-1} z: -116.34 cm^{-1}	x: 92.08 cm^{-1} y: -272.77 cm^{-1} z: -116.51 cm^{-1}
μ	0.233 Debye	0.256 Debye

III.

Table S4. Calculated bond lengths (Å) of the optimized S_0 and T_1 of compound **1** in gas phase and toluene solvent (the numbers in parentheses denote the ligands).

	In gas phase		In toluene	
	S_0-geom	T_1-geom	S_0-geom	T_1-geom
Ir-N(1)	2.1826	2.2093	2.1815	2.2081
Ir-C(1)	2.0426	2.0423	2.0430	2.0438
Ir-N(2)	2.1761	2.1486	2.1763	2.1498
Ir-C(2)	2.0312	1.9872	2.0318	1.9871
Ir-N(3)	2.1651	2.1713	2.1648	2.1691
Ir-C(3)	2.0482	2.0614	2.0486	2.0615

From Table S4, it is obvious that the gometry slight varies when going from in gas phase to toluene solvent. Based on the have optimized the S_0 and T_1 molecular geometries in gas phase and toluene solvent adopted in the experiments, the molecular reorganization energies were calculated to be 2213 cm^{-1} in gas phase and 2233 cm^{-1} in toluene, which are very close to each other. This indicates that the T_1 is insensitive to the solvent environment because its dipole moment (4.30 Debye) is similar to that of S_0 (5.16 Debye). Therefore, we neglected the solvent effect on the photophysical properties of the compounds investigated in the work.

IV.

Table S5. The orbital energy and molecular orbital composition (%) of FMOs at the ground state optimized geometries for compounds **1-5**.

1						
Orbitals	*E*(eV)	Ir-d	ppz-I-π	ppz-II-π	ppy-π	Bond nature
L	-1.1614	2.43	0.00	0.00	92.59	π*(ppy)
H	-4.9666	47.60	7.45	12.04	24.92	d(Ir) +π(ppy)+ π(ppz)
H-1	-4.9963	43.21	3.55	35.13	7.84	d(Ir) +π(ppy)+ π(ppz)
H-2	-5.0673	40.74	36.08	0.52	12.68	d(Ir) +π(ppy)+ π(ppz)
H-3	-5.8513	6.43	1.34	70.09	13.75	π(ppy)+π(ppz)
2						
Orbitals	*E*(eV)	Ir-d	F_2ppz-I-π	F_2ppz-II-π	F_2ppy-π	Bond nature
L	-1.4868	2.41	0.00	0.00	91.65	π*(F_2ppy)
H	-5.5421	45.82	8.74	12.63	23.50	d(Ir)+π(F_2ppz)+ π(F_2ppy)
H-1	-5.5672	41.42	7.40	35.76	6.74	d(Ir)+π(F_2ppz)+ π(F_2ppy)
H-2	-5.6436	38.51	37.32	0.00	13.64	d(Ir)+π(F_2ppz)+ π(F_2ppy)
H-3	-6.0907	6.49	49.15	12.60	25.22	π(F_2ppz) + π(F_2ppy)
3						
Orbitals	*E*(eV)	Ir-d	F_2ppz-I-π	F_2ppz-II-π	F_2ppz-III-π	Bond nature
L+2	-0.7867	3.12	7.62	19.63	59.87	π*(F_2ppz)
L+1	-0.7872	3.13	50.61	37.80	0.00	π*(F_2ppz)
L	-0.8555	1.04	29.39	29.66	29.35	π*(F_2ppz)
H	-5.6124	42.83	18.35	17.03	13.13	d(Ir)+π(F_2ppz)
H-1	-5.6249	38.85	9.02	1.64	28.27	d(Ir)+π(F_2ppz)
H-2	-5.6262	38.73	18.53	29.81	2.88	d(Ir)+π(F_2ppz)
H-3	-6.1158	8.61	51.99	30.82	0.00	π(F_2ppz)
H-4	-6.1166	8.60	3.93	24.28	55.23	π(F_2ppz)
H-5	-6.1805	12.30	25.90	26.35	26.41	π(F_2ppz)
4						
Orbitals	*E*(eV)	Ir-d	F_2ppz-I-π	F_2ppz-II-π	F_2pypy-π	Bond nature
L	-1.6599	2.47	0.00	0.00	91.56	π*(F_2pypy)
H	-5.7326	40.78	3.36	48.11	0.60	d(Ir)+ π(F_2ppz)
H-1	-5.7794	38.56	49.24	0.50	1.89	d(Ir)+ π(F_2ppz)
H-2	-5.9952	50.25	3.68	9.29	27.01	d(Ir)+ π(F_2ppz)+ π(F_2pypy)
H-3	-6.2314	10.08	10.10	73.50	0.00	π(F_2ppz)

H-4	-6.2622	9.04	57.56	4.42	20.56	π(F_2ppz) + π(F_2pypy)
H-5	-6.3996	5.70	14.81	0.00	70.08	π(F_2ppz)+ π(F_2pypy)

5

Orbitals	*E*(eV)	Ir-d	F_2pmpz I-π	F_2pmpz II-π	F_2pmpy-π	Bond nature
L	-2.0044	2.23	0.00	0.00	91.84	π*(F_2pmpy)
H	-6.3607	36.95	10.97	32.36	7.94	d(Ir)+ π(F_2pmpz)+ π(F_2pmpy)
H-1	-6.4214	33.28	19.67	23.64	12.06	d(Ir)+ π(F_2pmpz)+ π(F_2pmpy)
H-2	-6.5229	29.61	33.26	2.68	23.19	d(Ir)+ π(F_2pmpz)+ π(F_2pmpy)
H-3	-6.7904	0.99	16.21	24.72	29.42	π(F_2pmpz)+ π(F_2pmpy)
H-5	-7.0279	24.33	25.87	11.67	21.52	d(Ir)+ π(F_2pmpz)+ π(F_2pmpy)

Notes: H and L denote HOMO and LUMO, respectively.

V.

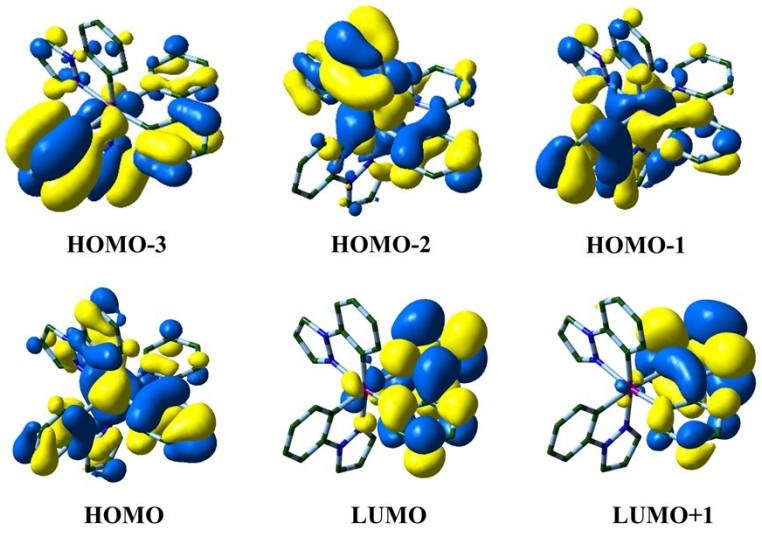

Compound 1

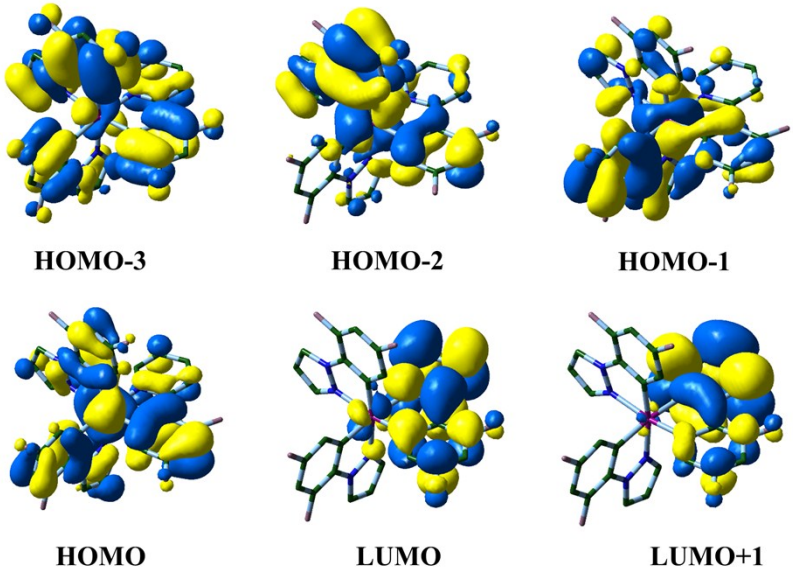

Compound 2

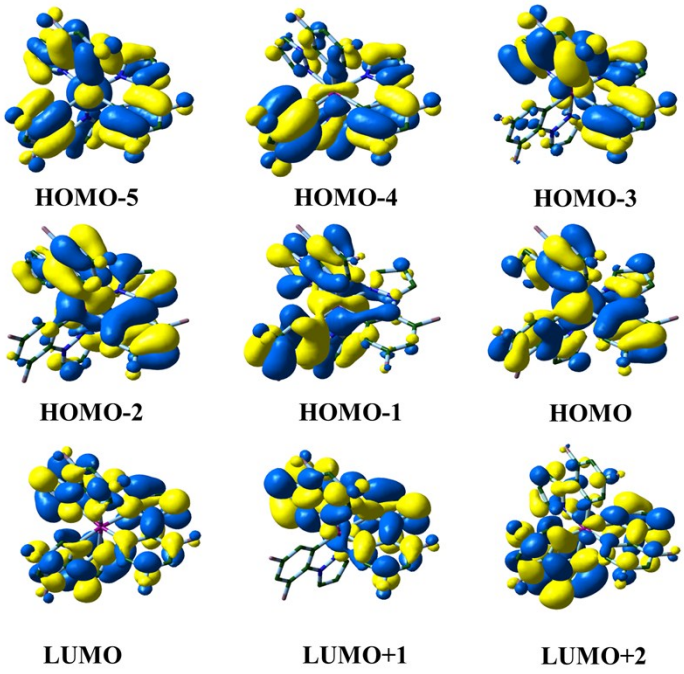

Compound 3

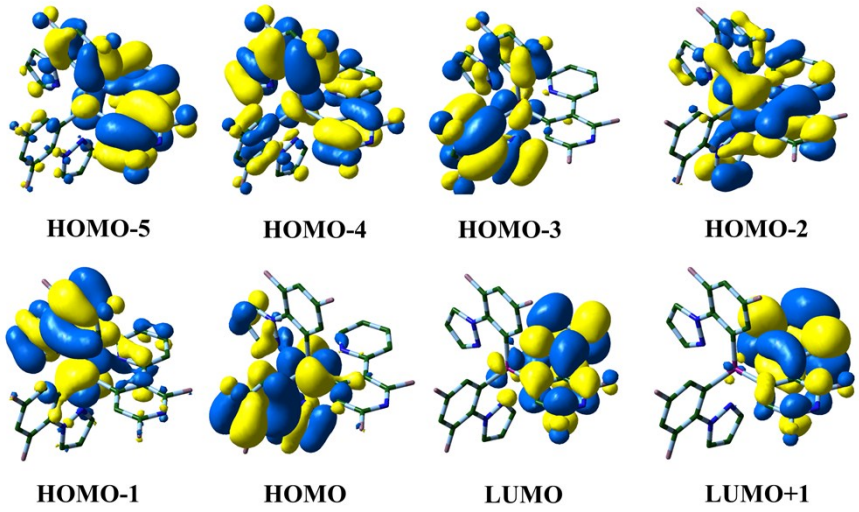

Compound 4

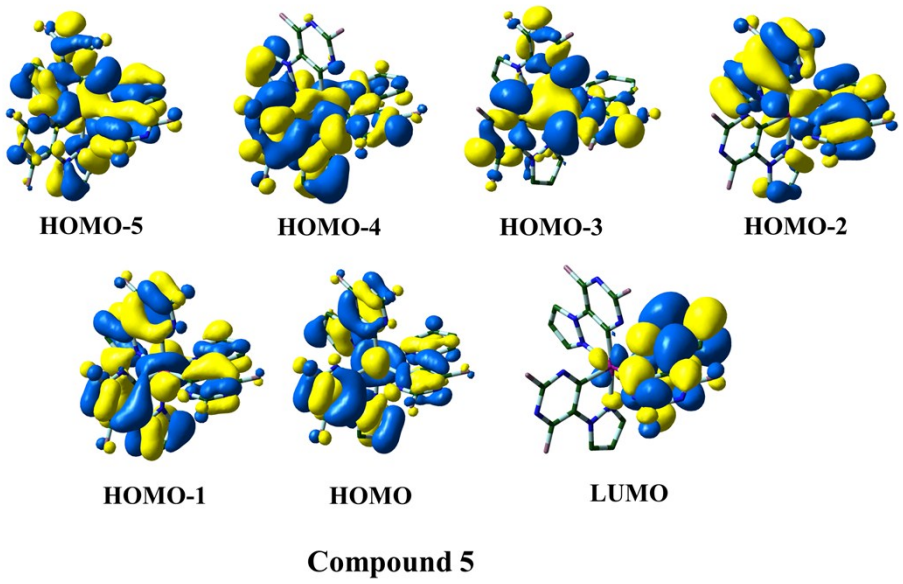

Figure S1. Profiles of the selected frontier molecular orbitals at the optimized ground-state geometries for **1-5**.

VI.

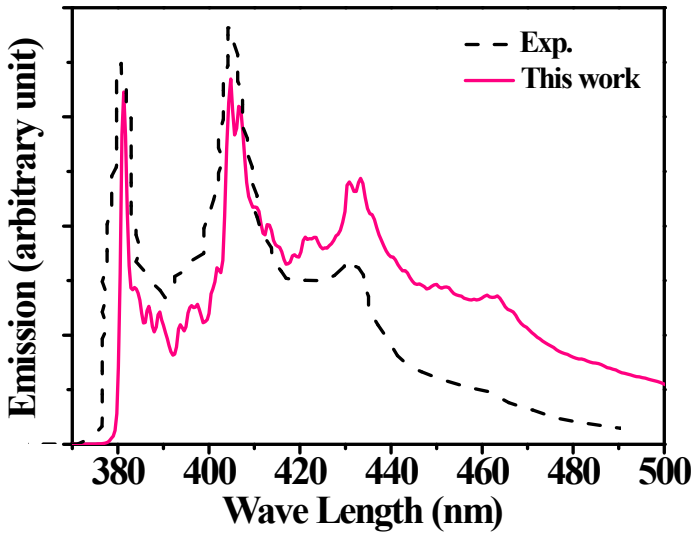

Figure S2. The comparison of the calculated and experimental spectra of **3** at 77 K.

VII.

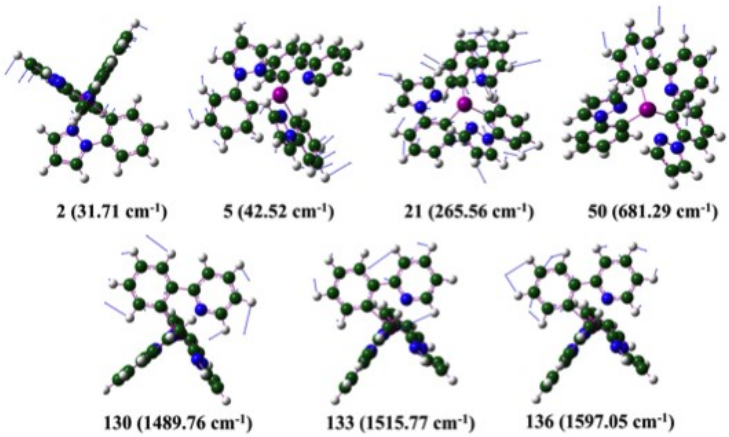

Compound 1

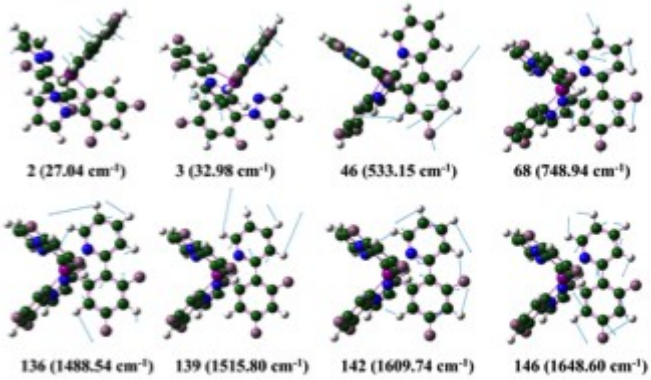

Compound 2

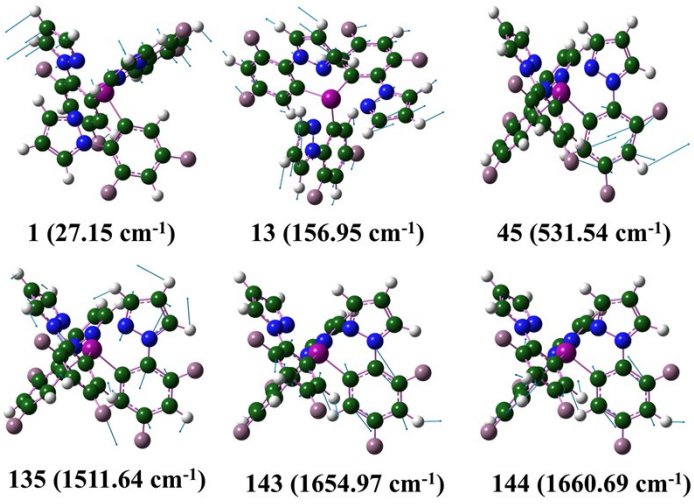

Compound 3

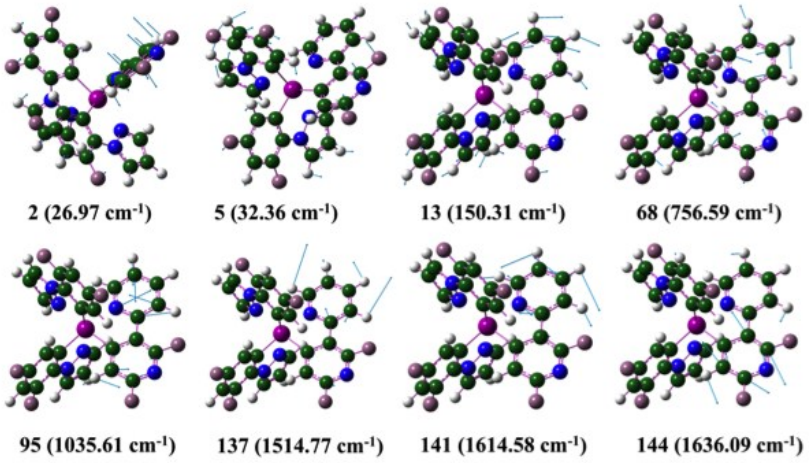

Figure S3. The displacement vectors of the vibration normal modes mainly involved in the emission spectra for **1-5**: index number (wavenumber)

VIII.

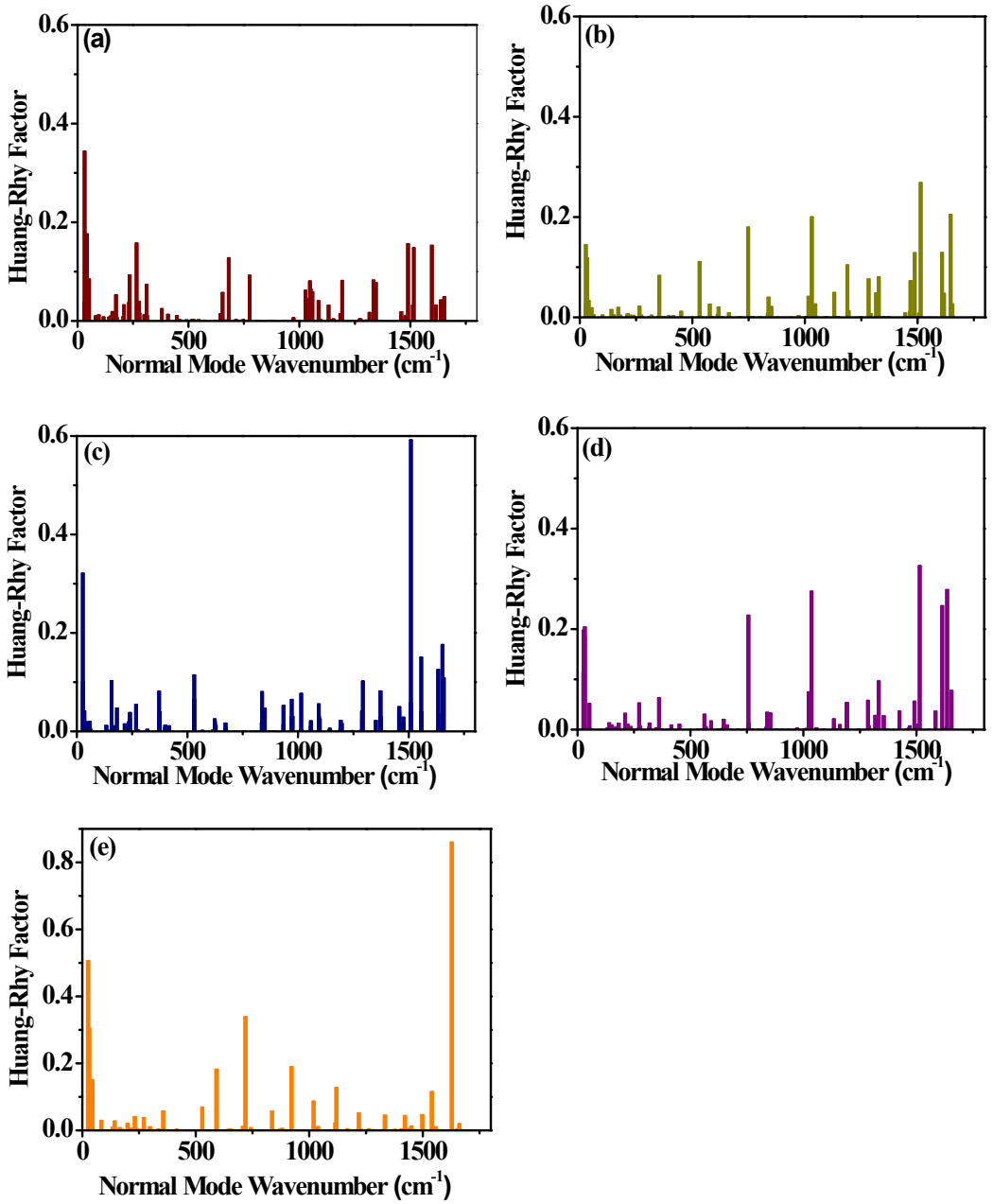

Figure S4. The calculated Huang-Rhys factors versus the normal mode wavenumber at the ground state for **1**-**5**.

VIIII.

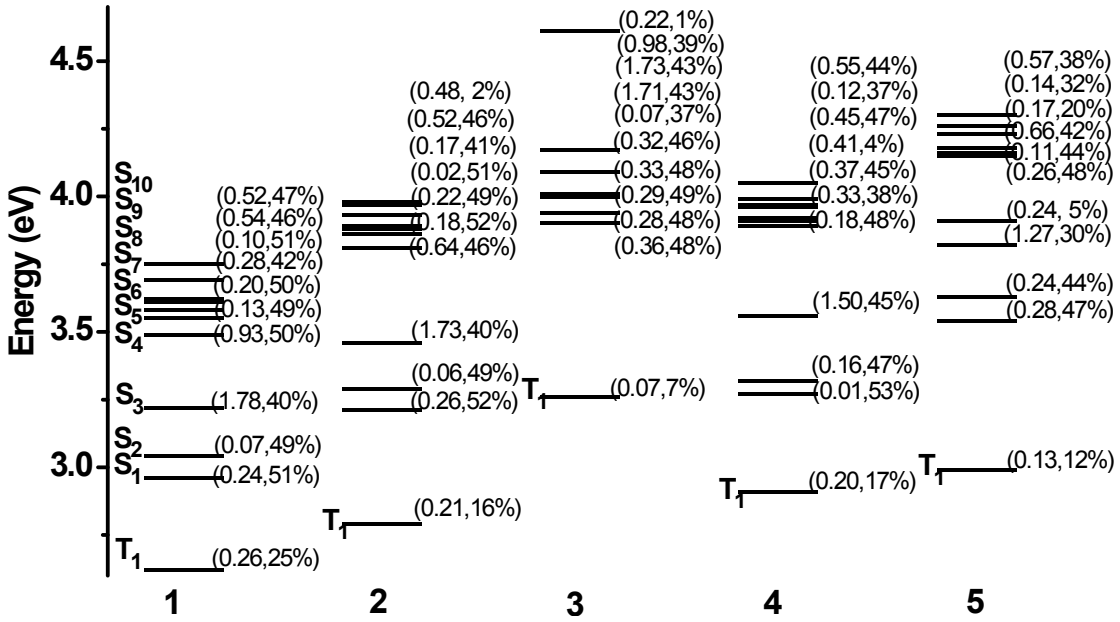

Figure S5. The transition energies (ΔE, eV), electric transition dipole moments (μ, Debye) and the Ir-d orbital components of the transition configurations with (μ, d%) for the lowest ten singlet states (S_n, n=1-10) and the first triplet state (T_1) at the ground-state optimized geometries for **1**-**5**.

X.

Based on the first-order perturbation, the formula of intersystem crossing can be represented as

$$k_{\mathrm{isc}} = \frac{1}{\mathsf{h}^2}\left|H^{\mathrm{SO}}\right|^2 \int_{-\infty}^{\infty} \mathrm{d}t \mathrm{e}^{\mathrm{i}\omega_{\mathrm{if}}t} Z_{\mathrm{i}}^{-1} \rho_{\mathrm{fi}}^{(0)}(t) \tag{S-10}$$

where the correlation function $\rho_{\mathrm{fi}}^{(0)}(t)$ is

$$\rho_{\mathrm{fi}}^{(0)}(t) = \mathrm{Tr}\left[\mathrm{e}^{-i\tau_{\mathrm{f}}\hat{H}^{\mathrm{f}}}\mathrm{e}^{-i\tau_{\mathrm{i}}\hat{H}^{\mathrm{i}}}\right] = \sqrt{\frac{\det\left[\mathbf{a}_{\mathrm{f}}\mathbf{a}_{\mathrm{i}}\right]}{\det\left[\mathbf{K}\right]}} \exp\left\{\frac{i}{\mathsf{h}}\left[-\frac{1}{2}\underline{F}^{\mathrm{T}}\mathbf{K}^{-1}\underline{F} + \underline{D}^{\mathrm{T}}\mathbf{E}\underline{D}\right]\right\} \tag{S-11}$$

where

$$\tau_{\mathrm{f}} = t/\mathsf{h} \tag{S-12}$$

$$\tau_{\mathrm{i}} = -t/\mathsf{h} - i\beta \tag{S-13}$$

$$a_{\mathrm{i/f},k}\left(\tau_{\mathrm{i/f}}\right) = \frac{\omega_{\mathrm{i/f},k}}{\sin\left(\mathsf{h}\omega_{\mathrm{i/f},k}\tau_{\mathrm{i/f}}\right)} \tag{S-14}$$

$$b_{\mathrm{i/f},k}\left(\tau_{\mathrm{i/f}}\right) = \frac{\omega_{\mathrm{i/f},k}}{\tan\left(\mathsf{h}\omega_{\mathrm{i/f},k}\tau_{\mathrm{i/f}}\right)} \tag{S-15}$$

$$\mathbf{A} = \mathbf{a}_{\mathrm{f}} + \mathbf{S}^{\mathrm{T}}\mathbf{a}_{\mathrm{i}}\mathbf{S} \tag{S-16}$$

$$\mathbf{B} = \mathbf{b}_{\mathrm{f}} + \mathbf{S}^{\mathrm{T}}\mathbf{b}_{\mathrm{i}}\mathbf{S} \tag{S-17}$$

$$\mathbf{E} = \mathbf{b}_{\mathrm{i}} - \mathbf{a}_{\mathrm{i}} \tag{S-18}$$

$$\underline{F}^{\mathrm{T}} = \begin{bmatrix} \underline{D}^{\mathrm{T}}\mathbf{E}\mathbf{S} \\ \underline{D}^{\mathrm{T}}\mathbf{E}\mathbf{S} \end{bmatrix} \tag{S-19}$$

$$\underline{F} = \begin{bmatrix} \mathbf{S}^{\mathrm{T}}\mathbf{E}\underline{D} \\ \mathbf{S}^{\mathrm{T}}\mathbf{E}\underline{D} \end{bmatrix} \tag{S-20}$$

$$\mathbf{K} = \begin{bmatrix} \mathbf{B} & -\mathbf{A} \\ -\mathbf{A} & \mathbf{B} \end{bmatrix} \tag{S-21}$$

In displaced oscillator model,

$$\mathbf{S} = \mathbf{I} \tag{S-22}$$

$$\omega_{\mathrm{i},k} = \omega_{\mathrm{f},k} \tag{S-23}$$

Then

$$b_{\mathrm{f},k}(\tau_{\mathrm{f}}) - a_{\mathrm{f},k}(\tau_{\mathrm{f}}) = -\omega_k \tan\frac{\mathsf{h}\omega_k\tau_{\mathrm{f}}}{2} \tag{S-24}$$

$$b_{\mathrm{f},k}(\tau_{\mathrm{f}}) + a_{\mathrm{f},k}(\tau_{\mathrm{f}}) = \omega_k \cot\frac{\mathsf{h}\omega_k\tau_{\mathrm{f}}}{2} \tag{S-25}$$

$$b_{\mathrm{i},k}(\tau_{\mathrm{i}}) - a_{\mathrm{i},k}(\tau_{\mathrm{i}}) = -\omega_k \tan\frac{\mathsf{h}\omega_k\tau_{\mathrm{i}}}{2} \tag{S-26}$$

And

$$\frac{i}{\mathsf{h}}\left\{-\frac{1}{2}\underline{F}^{\mathrm{T}}\mathbf{K}^{-1}\underline{F} + \underline{D}^{\mathrm{T}}\mathbf{E}\underline{D}\right\} = -\sum_k S_k\left[(2\overline{n}_k+1) - (\overline{n}_k+1)\mathrm{e}^{-i\omega_k t} - \overline{n}_k\mathrm{e}^{i\omega_k t}\right] \tag{S-27}$$

And

$$\frac{1}{Z_{\mathrm{i}}}\sqrt{\frac{\det\left[\mathbf{a}_{\mathrm{g}}\right]\det\left[\mathbf{a}_{\mathrm{e}}\right]}{\det\left[\mathbf{K}\right]}} = 1 \tag{S-28}$$

Here, $\overline{n}_k \equiv \dfrac{1}{\mathrm{e}^{\mathsf{h}\omega_k/k_{\mathrm{B}}T} - 1}$ is the average number of the photons.

So,

$$k_{\mathrm{isc}} \equiv \frac{1}{\mathsf{h}^2}\left|H^{\mathrm{SO}}\right|^2 \int_{-\infty}^{\infty} \mathrm{d}t F(t) \tag{S-29}$$

where

$$F(t) \equiv \exp\left\{i\omega_{\mathrm{if}}t - \sum_k S_k\left[(2\overline{n}_k+1) - (\overline{n}_k+1)\mathrm{e}^{-i\omega_k t} - \overline{n}_k\mathrm{e}^{i\omega_k t}\right]\right\} \tag{S-30}$$

The real part of the function $F(t)$is even, and the imaginary part is odd. The integral is determined by the real part. The integral result in eq.(VII-21) is unchangeable when the variable t is replaced by -t.

$$k_{\mathrm{isc}} = \frac{1}{\mathsf{h}^2}\left|H^{\mathrm{SO}}\right|^2 \int_{-\infty}^{\infty} \mathrm{d}t \exp\left\{i\omega_{\mathrm{fi}}t - \sum_k S_k\left[(2\overline{n}_k+1) - (\overline{n}_k+1)\mathrm{e}^{i\omega_k t} - \overline{n}_k\mathrm{e}^{-i\omega_k t}\right]\right\} \tag{S-31}$$

If $\sum_k S_k >> 1$， and the short time approximation is adopted

$$e^{\pm i\omega_k t} \approx 1 \pm i\omega_k t - \frac{1}{2}\omega_k^2 t^2 \tag{S-32}$$

The analytic solution can be obtained

$$k_{\text{isc}} = \frac{1}{\hbar^2}\left|H^{\text{SO}}\right|^2 \sqrt{\frac{2\pi}{\sum_k S_k \omega_k^2 \left(2\bar{n}_k + 1\right)}} \exp\left\{-\frac{\left(\omega_{\text{fi}} + \sum_k S_k \omega_k\right)^2}{2\sum_k S_k \omega_k^2 \left(2\bar{n}_k + 1\right)}\right\} \tag{S-33}$$

We can replace the frequency by the energy,

$$\bar{E}_k \equiv \left(\bar{n}_k + \frac{1}{2}\right)\hbar\omega_k \tag{S-34}$$

The final form is obtained

$$k_{\text{isc}}\left(E_{\text{if}}\right) = \frac{1}{\hbar}\left|H^{\text{SO}}\right|^2 \sqrt{\frac{\pi}{\sum_k \lambda_k \bar{E}_k}} \exp\left\{-\frac{\left(E_{\text{if}} - \sum_k \lambda_k\right)^2}{4\sum_k \lambda_k \bar{E}_k}\right\} \tag{S-35}$$

The broadening of Eq. (VII-27) is $\sum_k \lambda_k \bar{E}_k$. When $\sum_k \lambda_k \bar{E}_k$ increases, the energy gap function, the rate of intersystem crossing, $k_{\text{isc}}\left(E_{\text{if}}\right)$ becomes broader.

XI.

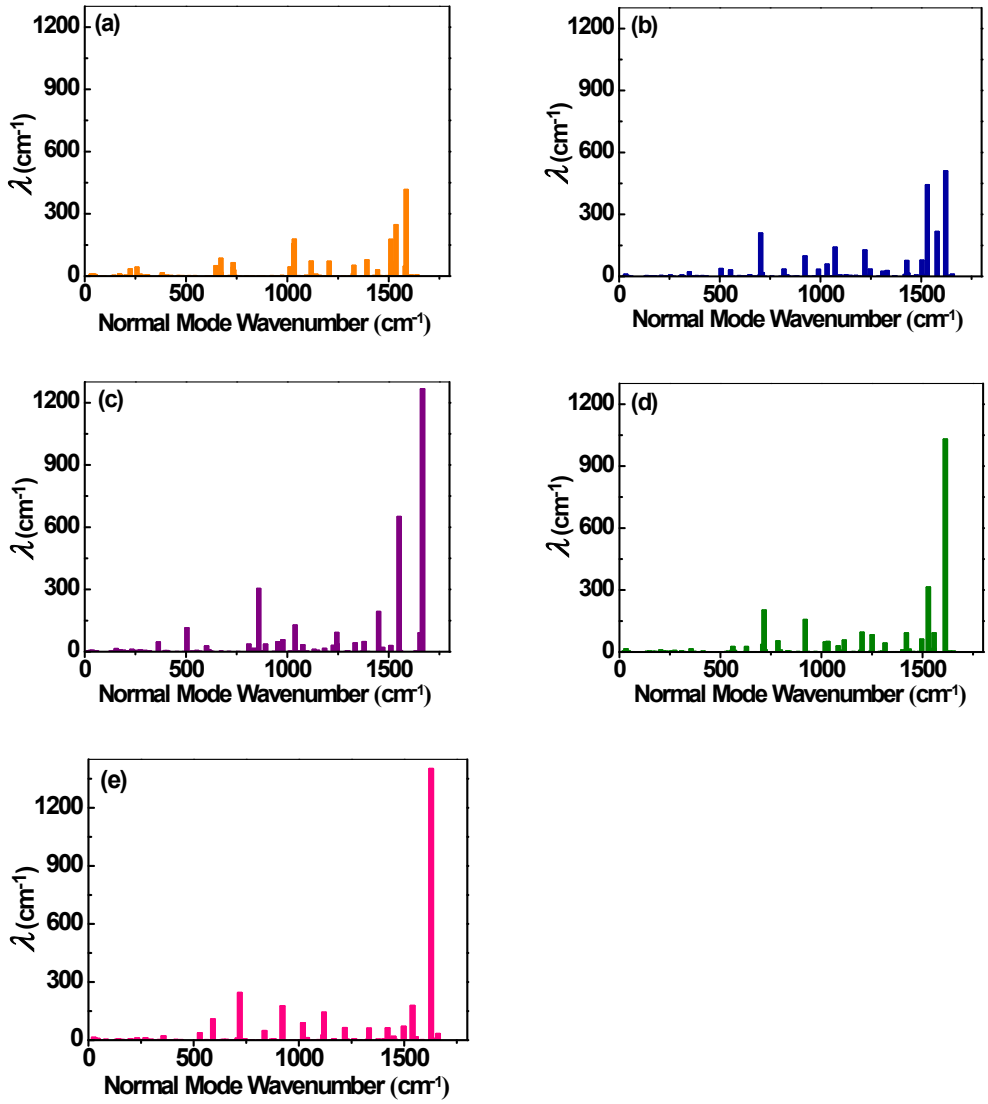

Figure S6. Reorganization energies versus the normal mode wavenumbers for **1**(a), **2**(b), **3**(c), **4**(d), and **5**(e).

XII.

Table S6. Selected reorganization energy λ_k (cm^{-1}) and the vibrational normal mode frequencies ω_k (cm^{-1}) for **1**-**5**.

1		**2**		**3**		**4**		**5**	
ω_k	λ_k	ω_k	λ_k	ω_k	λ_k	ω_k	λ_k	ω_k	λ_k
32.21	8.6	32.84	9.49	32.53	14.4	155.83	13.66	25.24	12.77
41.91	9.38	254.6	5.37	204.54	8.7	174.44	7.71	27.41	6.36
51.16	5.81	311.86	4.98	273.32	5.98	191.74	5.47	28.65	2.78
172.14	9.58	348.8	20.49	354.7	13.75	232.95	9.89	30.54	9.31
224.81	33.1	506.2	36.22	557.71	7.55	273.83	7.51	44.15	6.63
257.76	42.07	552.98	29.94	561.38	25	363.25	45.25	231.16	9.39
274.08	7.35	648.85	6.02	569.07	6.16	504.2	113.68	270.94	10.19
382.77	14.33	702.88	208.07	628.56	24.92	601.24	26.59	356.49	20.52
647.39	48.78	711.23	16.47	709.27	34.99	612.27	8.56	528.78	36.37
671.85	84.59	818.52	33.83	716.22	201.37	809.89	35.01	591.41	107.59
672.53	16.84	833.38	5.13	722.01	8.63	834.92	14.43	718.9	243.83
732.32	62.92	922.85	97.18	784.57	52.54	842.53	9.75	742.31	5.31
732.48	41.53	989.94	32.61	796.43	7.87	858.24	303.58	836.32	47.59
735.85	27.93	1032.55	58.05	919.69	156.09	891.99	35.28	921.82	175.38
1013.38	42.61	1072.66	139.78	1018.82	47.07	952.65	46.41	1019.07	88.45
1022.22	9.68	1097.68	5.6	1031.58	49.4	977.49	56.02	1038.58	10.93
1031.1	154.71	1127.23	6.36	1082.83	27.88	1038.29	126.9	1115.11	24.91
1034.31	176.08	1220.21	125.83	1098.96	6.81	1075.74	31.88	1119.37	142.63
1117.44	70.89	1246.91	33.54	1113.16	56.09	1132.32	10.05	1218.28	62.52
1141.51	7.71	1308.98	22.5	1195.05	7.04	1183.43	14.26	1262.84	5.5
1206.41	69.58	1331.06	26.89	1200.93	94.58	1226.92	29.2	1333.27	59.84
1324.98	10.46	1420.71	7.67	1250.65	81.86	1243.63	91.45	1421.31	62.23
1328.04	49.85	1428.03	75.11	1314.84	42.13	1244.86	36.47	1435.63	6.54
1392.51	77.08	1433.47	14.2	1401.65	8.57	1334.6	41.35	1449.72	17.68
1444.89	28.59	1475.83	4.98	1420.27	91.01	1378.63	47.14	1497.93	69.76
1510.7	175.91	1503.66	76.97	1434.27	12.3	1450.14	192.68	1539.96	177.51
1512.66	59.38	1507.24	7.76	1495.69	60.93	1456.33	12.47	1555.80	15.17
1514.18	66.59	1530.62	442.08	1529.1	313.54	1465.54	13.75	1628.26	1400.69
1535.9	246.36	1579.38	216.2	1556.86	16.82	1470.26	19.32	1652.24	6.62
1581.61	46.1	1621.12	509.33	1557.33	91.44	1510.49	27.89	1661.26	32.12
				1613.17	1029.42	1551.70	650.28		
						1655.20	89.68		

XIII.

Table S7. the selected bond lengths (Å), angles (°) and dihedral angles (°) of the S_0 and T_1 states and the corresponding modification between the two states for **1**.

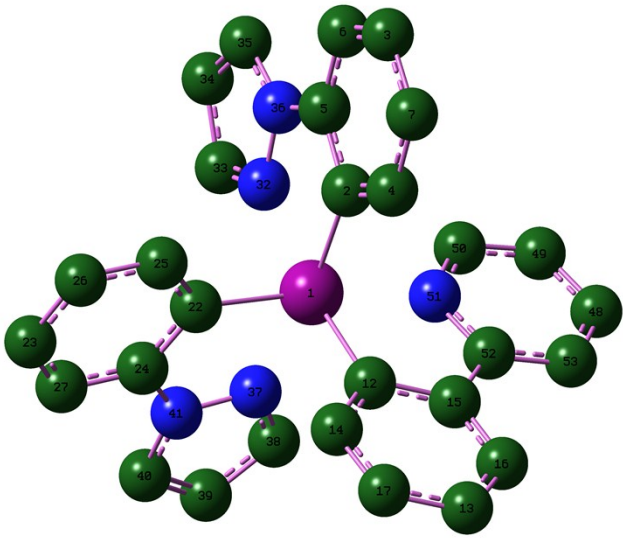

	S_0	T_1	$\Delta(T_1-S_0)$		S_0	T_1	$\Delta(T_1-S_0)$
				ppz-I			
L(Ir1-C2)	2.043	2.042	-0.001	A(C2-C5-C6)	123.86	123.54	-0.31
L(Ir1-N32)	2.183	2.210	0.027	A(C6-C3-C7)	119.40	119.45	0.05
L(C5-C2)	1.416	1.414	-0.002	A(Ir1-C2-C5)	115.98	116.33	0.35
L(C7-C3)	1.397	1.397	0.000	A(C6-C5-N36)	120.39	120.38	-0.01
L(N36-N32)	1.357	1.355	-0.002	A(C33-N32-N36)	106.68	106.77	0.09
L(C5-N36)	1.428	1.427	-0.001	D(Ir1-C2-C5-N36)	0.28	0.33	0.05
L(C34-C35)	1.385	1.385	0.000	D(C4-C2-C5-N36)	-179.88	-179.90	-0.02
				ppy			
L(Ir1-C12)	2.031	1.987	-0.044	A(C12-C15-C16)	121.27	118.51	-2.76
L(Ir1-N51)	2.176	2.149	-0.027	A(C16-C13-C17)	119.19	121.65	2.46
L(C15-C12)	1.427	1.492	0.065	A(Ir1-C12-C15)	115.67	113.87	-1.80
L(C17-C13)	1.400	1.429	0.029	A(C16-C15-C52)	122.34	124.24	-1.90
L(C52-N51)	1.365	1.416	0.051	A(C50-N51-C52)	120.05	119.16	-0.89
L(C52-C15)	1.466	1.407	-0.059	D(Ir1-C12-C15-C52)	0.60	-1.02	-1.82
L(C49-C48)	1.398	1.428	0.030	D(C14-C12-C15-C52)	-179.70	-178.78	-0.92
				ppz-II			
L(Ir1-C22)	2.048	2.061	0.013	A(Ir1-C22-C24)	115.71	115.40	-0.31
L(Ir1-N37)	2.165	2.171	0.006	A(C22-C24-C27)	123.93	123.82	-0.11
L(C24-C22)	1.416	1.414	-0.002	A(C27-C23-C26)	119.40	119.50	0.10
L(C23-C26)	1.397	1.397	0.000	A(C27-C24-N41)	120.47	120.37	-0.10
L(N41-N37)	1.357	1.358	0.001	A(C38-N37-N41)	106.72	106.92	0.20
L(N41-C24)	1.428	1.430	0.002	D(Ir1-C22-C24-N41)	0.53	0.81	0.28
L(C40-C39)	1.385	1.386	0.001	D(C25-C22-C24-N41)	-179.71	-179.98	-0.27

Table S8. the selected bond lengths (Å), angles (°) and dihedral angles (°) of the S_0 and T_1 states and the corresponding modification between the two states for **2**.

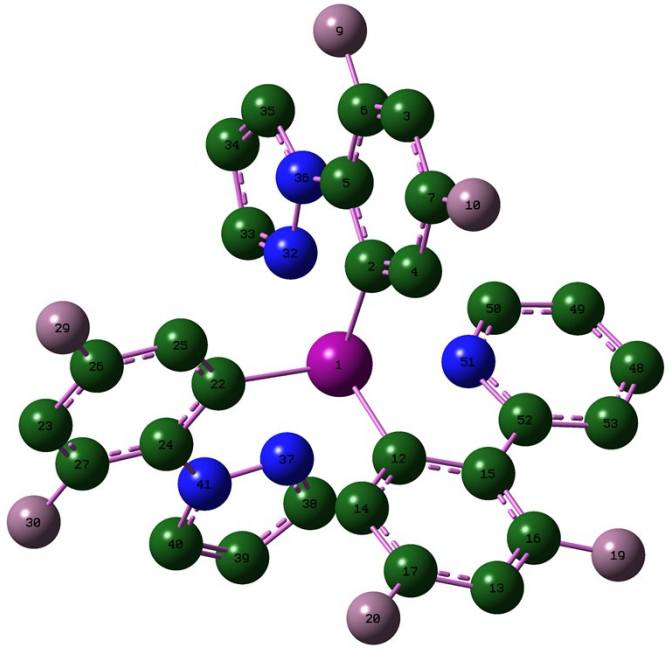

	S_0	T_1	$\Delta(T_1-S_0)$		S_0	T_1	$\Delta(T_1-S_0)$
				F_2ppz-I			
L(Ir1-C2)	2.041	2.039	-0.002	A(C2-C5-C6)	121.20	121.00	-0.20
L(Ir1-N32)	2.174	2.186	0.012	A(C6-C3-C7)	116.85	116.93	0.08
L(C5-C2)	1.420	1.419	-0.001	A(Ir1-N32-C33)	140.06	140.25	0.19
L(C6-C5)	1.395	1.395	0.000	A(C6-C5-N36)	122.14	122.16	0.02
L(N36-N32)	1.360	1.359	-0.001	A(C33-N32-N36)	106.64	106.69	0.05
L(C5-N36)	1.423	1.422	-0.001	D(Ir1-C2-C5-N36)	0.16	0.50	0.34
L(C34-C35)	1.385	1.384	-0.001	D(C4-C2-C5-N36)	-179.85	-179.76	0.09
				F_2ppy			
L(Ir1-C12)	2.030	2.005	-0.025	A(C12-C15-C16)	118.50	116.51	-1.99
L(Ir1-N51)	2.167	2.130	-0.037	A(C16-C13-C17)	116.80	118.41	1.61
L(C15-C12)	1.434	1.491	0.057	A(Ir1-N51-C50)	124.98	127.30	2.32
L(C16-C15)	1.405	1.443	0.038	A(C16-C15-C52)	124.65	125.69	1.04
L(C52-N51)	1.366	1.433	0.067	A(C50-N51-C52)	120.23	118.98	-1.25
L(C52-C15)	1.466	1.402	-0.064	D(Ir1-C12-C15-C52)	0.80	-0.16	-0.96
L(C49-C48)	1.396	1.432	0.036	D(C14-C12-C15-C52)	-179.53	-179.48	0.05
				F_2ppz-II			
L(Ir1-C22)	2.047	2.059	0.012	A(Ir1-N37-C38)	139.67	139.63	-0.04
L(Ir1-N37)	2.157	2.165	0.008	A(C22-C24-C27)	121.27	121.17	-0.10
L(C24-C22)	1.419	1.418	-0.001	A(C27-C23-C26)	116.84	116.92	0.08
L(C24-C27)	1.395	1.395	0.000	A(C27-C24-N41)	122.21	122.11	-0.10
L(N41-N37)	1.360	1.361	0.001	A(C38-N37-N41)	106.68	106.81	0.13
L(N41-C24)	1.422	1.424	0.002	D(Ir1-C22-C24-N41)	0.59	0.64	0.05
L(C40-C39)	1.384	1.385	0.001	D(C25-C22-C24-N41)	-179.59	-179.89	-0.30

Table S9. the selected bond lengths (Å), angles (°) and dihedral angles (°) of the S_0 and T_1 states and the corresponding modification between the two states for **3**.

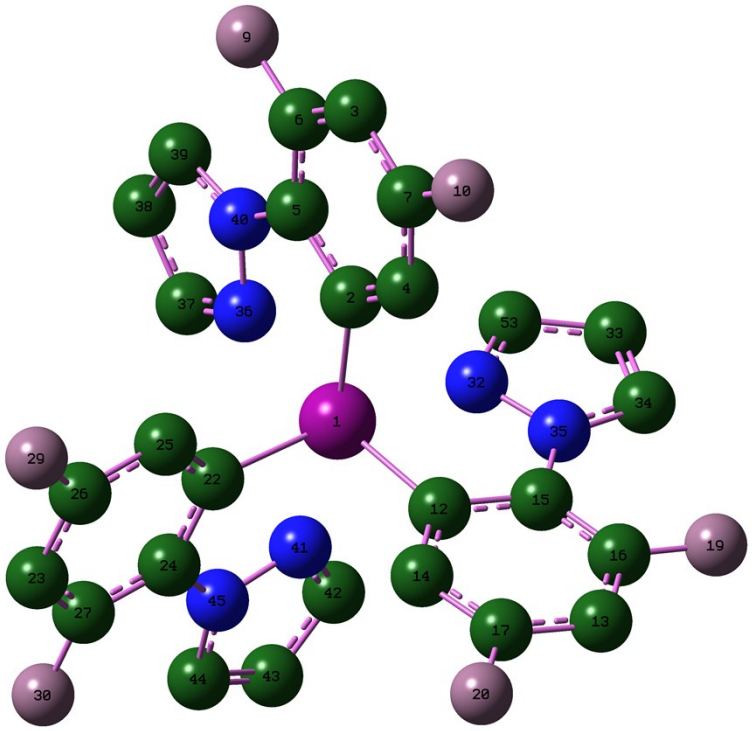

	S_0	T_1	$\Delta(T_1-S_0)$		S_0	T_1	$\Delta(T_1-S_0)$
				F_2ppz-I			
L(Ir1-C2)	2.042	2.051	0.009	A(Ir1-C2-C4)	128.39	128.38	-0.01
L(Ir1-N36)	2.159	2.166	0.007	A(C37-C38-C39)	105.31	105.30	-0.01
L(C5-C2)	1.420	1.419	-0.001	A(C2-C5-C6)	121.20	121.16	-0.04
L(C6-C5)	1.395	1.395	0.000	A(C7-C3-C6)	116.86	116.89	0.03
L(N36-N40)	1.360	1.360	0.000	A(C39-N40-N36)	110.34	110.27	-0.07
L(C5-N40)	1.422	1.424	0.002	D(Ir1-C2-C5-N40)	0.33	0.11	-0.22
L(C7-C3)	1.391	1.390	-0.001	D(C4-C2-C5-N40)	-179.81	-179.81	0.00
				F_2ppz-II			
L(Ir1-C12)	2.041	2.040	-0.001	A(Ir1-C12-C14)	128.42	128.16	-0.26
L(Ir1-N32)	2.158	2.169	0.011	A(C53-C33-C34)	105.30	105.31	0.01
L(C15-C12)	1.420	1.419	-0.001	A(C12-C15-C16)	121.19	121.12	-0.07
L(C16-C15)	1.395	1.395	0.000	A(C17-C13-C16)	116.87	116.84	-0.03
L(N32-N35)	1.360	1.359	-0.001	A(C34-N35-N32)	110.35	110.35	0.00
L(N35-C15)	1.422	1.422	0.000	D(Ir1-C12-C15-N35)	0.34	0.75	0.41
L(C17-C13)	1.391	1.390	-0.001	D(C14-C12-C15-N35)	-179.72	-179.48	0.24
				F_2ppz-III			
L(Ir1-C22)	2.041	2.006	-0.035	A(Ir1-C22-C25)	128.41	130.24	1.83
L(Ir1-N41)	2.159	2.145	-0.014	A(C42-C43-C44)	105.31	107.14	1.83
L(C24-C22)	1.419	1.504	0.085	A(C22-C24-C27)	121.21	119.48	-1.73
L(C24-C27)	1.395	1.452	0.057	A(C26-C23-C27)	116.85	118.46	1.61
L(N45-N41)	1.360	1.400	0.040	A(C44-N45-N41)	110.33	109.38	-0.95
L(N45-C24)	1.422	1.339	-0.083	D(Ir1-C22-C24-N45)	0.43	-1.34	-1.77
L(C26-C23)	1.391	1.431	0.040	D(C25-C22-C24-N45)	-179.68	-179.04	0.64

Table S10. the selected bond lengths (Å), angles (°) and dihedral angles (°) of the S_0 and T_1 states and the corresponding modification between the two states for **4**.

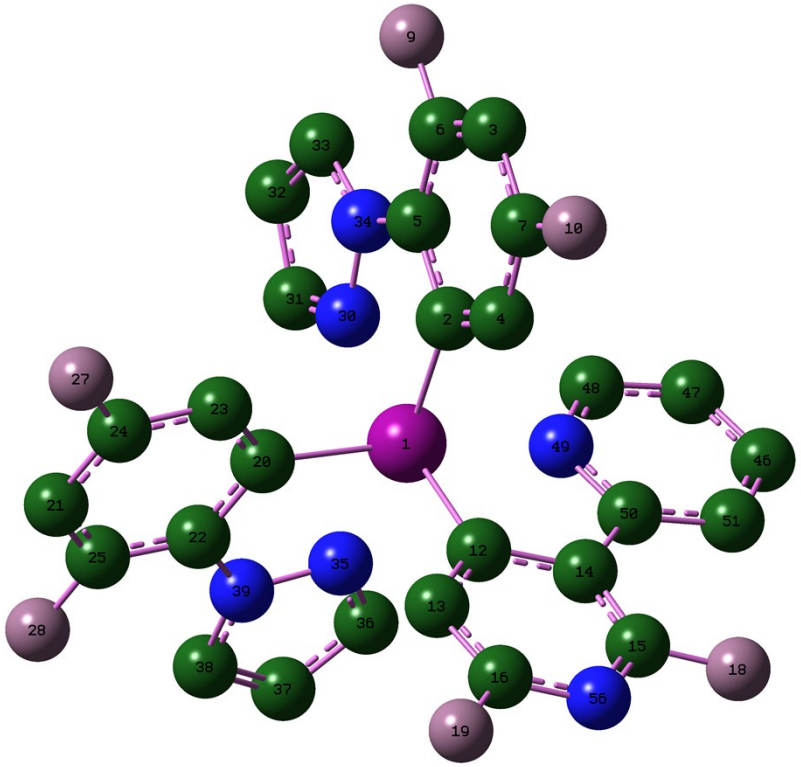

	S_0	T_1	$\Delta(T_1-S_0)$		S_0	T_1	$\Delta(T_1-S_0)$
				F_2ppz-I			
L(Ir1-C2)	2.043	2.037	-0.006	A(Ir1-C2-C4)	128.22	127.94	-0.28
L(Ir1-N30)	2.172	2.178	0.006	A(C31-C32-C33)	105.29	105.30	0.01
L(C5-C2)	1.419	1.420	0.001	A(C2-C5-C6)	121.17	120.96	0.21
L(C6-C5)	1.395	1.395	0.000	A(C7-C3-C6)	116.88	117.02	0.14
L(N30-N34)	1.360	1.360	0.000	A(C33-N34-N30)	110.37	110.36	-0.01
L(C5-N34)	1.423	1.421	-0.002	D(Ir1-C2-C5-N34)	0.16	0.46	-0.30
L(C7-C3)	1.391	1.391	0.000	D(C4-C2-C5-N34)	-179.81	-179.79	-0.02
				F_2pypy			
L(Ir1-C12)	2.018	2.013	-0.005	A(Ir1-C12-C14)	115.34	113.70	-1.64
L(Ir1-N49)	2.174	2.122	-0.052	A(C48-C47-C46)	118.03	118.43	0.10
L(C14-C12)	1.433	1.474	0.041	A(C12-C14-C15)	117.21	121.12	3.91
L(C14-C15)	1.401	1.450	0.049	A(C15-C56-C16)	115.62	115.26	-0.36
L(C15-N56)	1.313	1.297	0.016	A(C49-N50-N51)	119.59	118.43	-1.16
L(C46-C51)	1.389	1.363	0.026	D(Ir1-C12-C14-N50)	0.77	0.03	-0.44
L(C14-C50)	1.465	1.397	-0.068	D(C13-C12-C14-C50)	-179.53	-179.36	-0.17
				F_2ppz-II			
L(Ir1-C20)	2.047	2.060	0.013	A(Ir1-C20-C22)	114.96	114.91	-0.05
L(Ir1-N35)	2.157	2.168	0.011	A(C36-C37-C38)	105.30	105.33	0.03
L(C25-C22)	1.395	1.395	0.000	A(C20-C22-C25)	121.23	121.17	-0.06
L(C20-C22)	1.419	1.418	-0.001	A(C24-C21-C25)	116.87	116.91	0.04
L(N35-N39)	1.361	1.360	-0.001	A(N35-N39-C38)	110.34	110.25	-0.09
L(N39-C38)	1.361	1.361	0.000	D(Ir1-C20-C22-N39)	0.61	0.57	-0.04
L(C21-C25)	1.386	1.386	0.000	D(C23-C20-C22-N39)	-179.54	-179.72	0.18

Table S11. the selected bond lengths (Å), angles (°) and dihedral angles (°) of the S_0 and T_1 states and the corresponding modification between the two states for **5**.

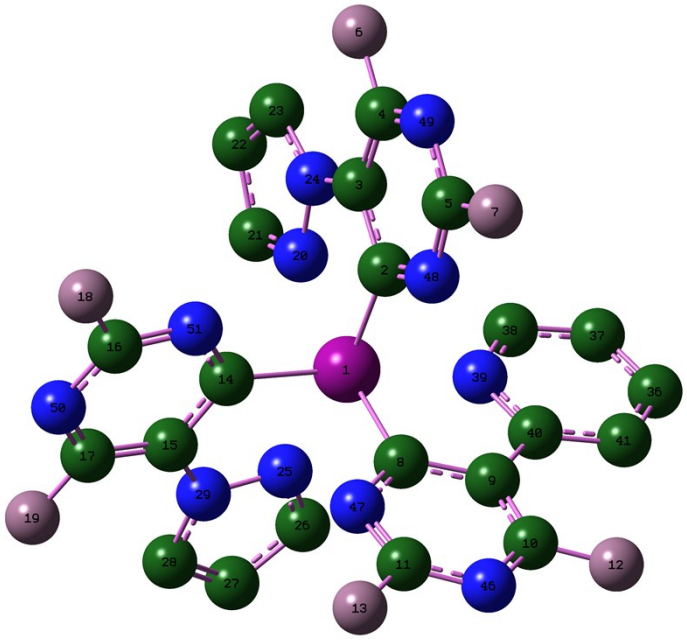

	S_0	T_1	$\Delta(T_1-S_0)$		S_0	T_1	$\Delta(T_1-S_0)$
				F_2pmpz-I			
L(Ir1-C2)	2.009	2.008	-0.001	A(Ir1-C2-N48)	126.12	125.84	-0.28
L(Ir1-N20)	2.203	2.212	0.009	A(N48-C5-N49)	129.22	129.10	-0.12
L(C3-C2)	1.421	1.420	-0.001	A(C2-C3-C4)	117.72	117.56	-0.16
L(C3-C4)	1.385	1.386	0.001	A(C3-C4-N49)	123.49	123.50	0.01
L(N20-N24)	1.362	1.362	0.000	A(C23-N24-N20)	110.71	110.69	-0.01
L(C3-N24)	1.413	1.413	0.000	D(Ir1-C2-C3-N24)	-1.77	-1.37	0.50
L(C4-N49)	1.315	1.315	0.000	D(N48-C2-C3-N24)	177.86	178.05	0.19
				F_2pmpy			
L(Ir1-C8)	1.999	1.984	-0.015	A(Ir1-C8-N47)	124.48	126.12	1.64
L(Ir1-N39)	2.192	2.160	-0.032	A(C8-C9-C40)	117.44	118.60	0.56
L(C8-C9)	1.431	1.488	0.057	A(C8-C9-C10)	115.38	113.27	-2.11
L(C9-C40)	1.461	1.390	-0.071	A(C10-N46-C11)	113.95	115.47	1.52
L(C40-N39)	1.365	1.437	0.072	A(N39-N40-C41)	119.90	118.81	-1.09
L(C8-N47)	1.347	1.328	-0.019	D(Ir1-C8-C9-C40)	-2.09	-6.60	-4.51
L(C10-N46)	1.315	1.295	-0.020	D(N47-C8-C9-C40)	177.06	172.75	-4.31
				F_2pmz-II			
L(Ir1-C14)	2.015	2.023	0.008	A(Ir1-C14-C15)	115.36	115.30	-0.06
L(Ir1-N25)	2.186	2.192	0.006	A(C14-C15-N29)	117.13	117.23	0.1
L(C14-C15)	1.421	1.420	-0.001	A(C14-C15-C17)	117.76	117.75	-0.01
L(C15-N29)	1.412	1.413	0.001	A(N51-C16-N50)	129.24	129.19	-0.05
L(N29-N25)	1.362	1.362	0.000	A(N25-N29-C15)	116.32	116.45	0.13
L(N51-C14)	1.347	1.347	0.000	D(Ir1-C14-C15-N29)	-1.78	-1.41	-0.37
L(C17-N50)	1.316	1.315	-0.001	D(N25-N29-C15-C17)	177.35	177.10	-0.25